

Rapid Communications

The *Rapid Communications* section is intended for the accelerated publication of important new results. Manuscripts submitted to this section are given priority in handling in the editorial office and in production. A Rapid Communication may be no longer than 3½ printed pages and must be accompanied by an abstract. Page proofs are sent to authors, but, because of the rapid publication schedule, publication is not delayed for receipt of corrections unless requested by the author.

Need for new physics in statistical models of nuclear deexcitation

Giovanni La Rana,^(a) David J. Moses,^(a) Winifred E. Parker,^(a) Morton Kaplan,^(a)
Douglas Logan,^(b) Roy Lacey,^(c) John M. Alexander,^(c) and Robert J. Welberry^(a)

^(a)Department of Chemistry, Carnegie-Mellon University, Pittsburgh, Pennsylvania 15213

^(b)Lawrence Berkeley Laboratory, Berkeley, California 94720

^(c)Department of Chemistry, State University of New York, Stony Brook, New York 11794

(Received 4 August 1986)

We have measured energy spectra and angular distributions of ^1H and ^4He from 190-MeV $^{40}\text{Ar} + ^{27}\text{Al}$ reactions. Comparisons with statistical model calculations show that evaporation from spherical nuclei cannot account for both the energy spectra and angular distributions, using entrance channel spins and evaporation barriers derived from fusion data. Alterations are required in both the emission barriers and the moments of inertia. Extensive nuclear deformation could explain the ^4He data, but discrepancies remain with the ^1H spectra, suggesting that additional effects are needed in the models.

The emergence of new and upgraded high-performance heavy-ion accelerators at laboratories around the world has triggered a surge in new experiments to explore the behavior of very hot nuclei. A natural course for such investigations is to extend our current ideas about hot nuclei to new regimes of energy, mass, and angular momentum, and to determine experimentally when and how our theoretical descriptions must be changed to embrace new observations. A focal point in these endeavors is the elucidation of the time scales and the extent to which the relevant degrees of freedom are equilibrated. The familiar signatures of energy sharing and thermal equilibrium are well understood in terms of statistical models of nuclear deexcitation,¹⁻³ as are the basic ideas involving spin effects.⁴ The success of statistical theories has led to the development of a number of sophisticated computer codes which are widely used for calculating nuclear evaporation properties: neutron and charged-particle spectra, multiplicities, cross sections, residue velocities and yields, photon distributions, etc. As these codes are rapidly finding applications in uncharted waters it is important to have a clear view of the weaknesses and potential difficulties of the basic model, in order that we do not confuse new phenomena with old, but perhaps unrecognized, shortcomings.

The objective of this Communication is to show that statistical model predictions for spherical nuclei are often at odds with the behavior of real nuclei heated to temperatures of only a few MeV. We report results for a typical system, $^{40}\text{Ar} + ^{27}\text{Al} \rightarrow ^{67}\text{Ga}^*$, for which we demonstrate that the bulk of the $^1\text{H}/^4\text{He}$ emission is due to essentially pure evaporative decay of compound nuclei. We then give

a detailed comparison of the data with standard statistical model calculations and highlight the nature of the observed discrepancies.

Energy spectra and angular distributions of ^1H and ^4He were measured from 190-MeV $^{40}\text{Ar} + ^{27}\text{Al}$ reactions. The experiment was carried out in reversed kinematics in order to obtain high quality evaporative particle spectra in the forward hemisphere while simultaneously discriminating against any direct particle emission.⁵ The target was a self-supporting $420 \mu\text{g}/\text{cm}^2$ Al foil, and the charged particles ($^1\text{H}/^4\text{He}$) were detected in a series of three-element (50, 500, 5000 μm) Si telescopes. The composite system $^{67}\text{Ga}^*$ was formed at an excitation energy of 91 MeV, and the critical angular momentum for fusion l_{crit} is $\sim 46\hbar$ as derived from fusion cross-section data.⁶ In this experiment we also used a large position-sensitive avalanche detector backed by an ionization chamber to measure evaporation residues and projectilelike fragments and to estimate the charged-particle multiplicities associated with each. At this energy, less than 1% of the $^1\text{H}/^4\text{He}$ arises from reactions with projectilelike survivors, and hence the inclusive data presented here are not biased by emissions from such fragments.

We show in Fig. 1 a pair of velocity contour maps of the invariant (particle) cross sections in order to provide an overall picture of the reaction pattern. Figure 1(a) is for ^1H emission and Fig. 1(b) is for ^4He emission. The circular arcs are all centered on the c.m. velocity (as indicated by $V_{\text{c.m.}}$ in Fig. 1). These circles do quite a good job of describing both the ^1H and ^4He data. Small deviations from the circles can be seen in the very forward and back-

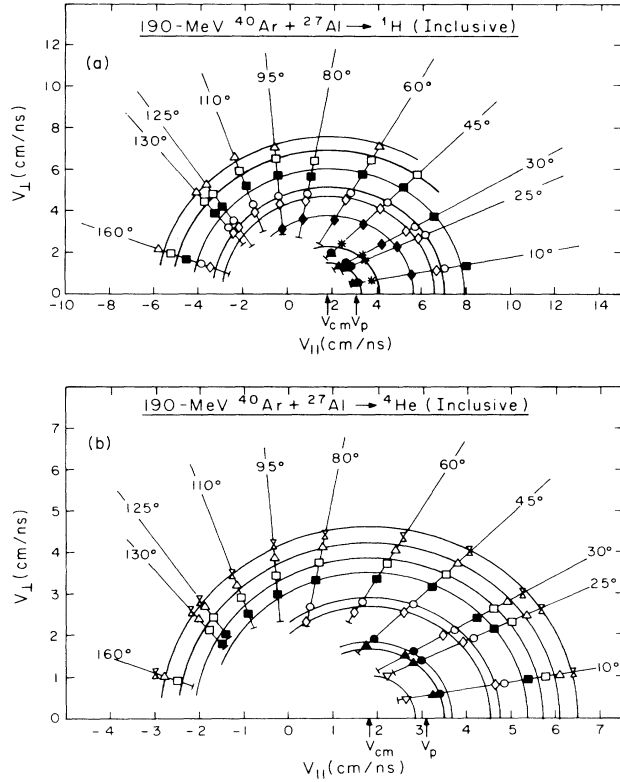


FIG. 1. Contour maps of the invariant cross section $(d^2\sigma/d\Omega d\epsilon)p^{-1}c^{-1}$ in units of $(\text{mb}/\text{sr MeV}^2)$ for (a) ^1H emission and (b) ^4He emission. The axes V_{\parallel} and V_{\perp} denote laboratory velocity components parallel and perpendicular to the beam, respectively. The circular arcs are centered on $V_{c.m.}$, the velocity of the center of mass, and the projectile velocity is V_p . Straight lines are drawn along the laboratory angles and terminated at the detector thresholds. The invariant cross section magnitudes are \times : 1×10^{-6} ; \triangle : 1×10^{-5} ; \square : 1×10^{-4} ; \blacksquare : 1×10^{-3} ; \circ : 1×10^{-2} ; \diamond : 2×10^{-2} ; \blacklozenge : 1×10^{-1} ; $*$: 1×10^{-1} ; \bullet : 2×10^{-2} ; \blacktriangle : 1×10^{-2} ; ∇ : 1×10^{-3} .

ward directions, and these are attributable to angular anisotropies in evaporative decay that result from the spins of the composite nuclei. Particle emission from direct or preequilibrium processes would appear as strong deviations from the circles in the direction of the light reaction partner (backward for reversed kinematics), and such effects are not prominent here. Thus we are confident that essentially all of the observed $^1\text{H}/^4\text{He}$ particles (particularly in the forward hemisphere) are associated with composite nucleus decay. The energy spectra of these particles (to be discussed below) are also strongly supportive of this conclusion.

Laboratory energy spectra are given in Fig. 2 at four angles as indicated. The points with occasional error bars are the experimental data. These spectra exhibit the characteristic features normally associated with compound nucleus evaporation: steeply rising at low energies, approximately exponential falloff at high energies with low apparent temperatures, and only slight (spin-driven) variations with angle. We have attempted to reproduce these

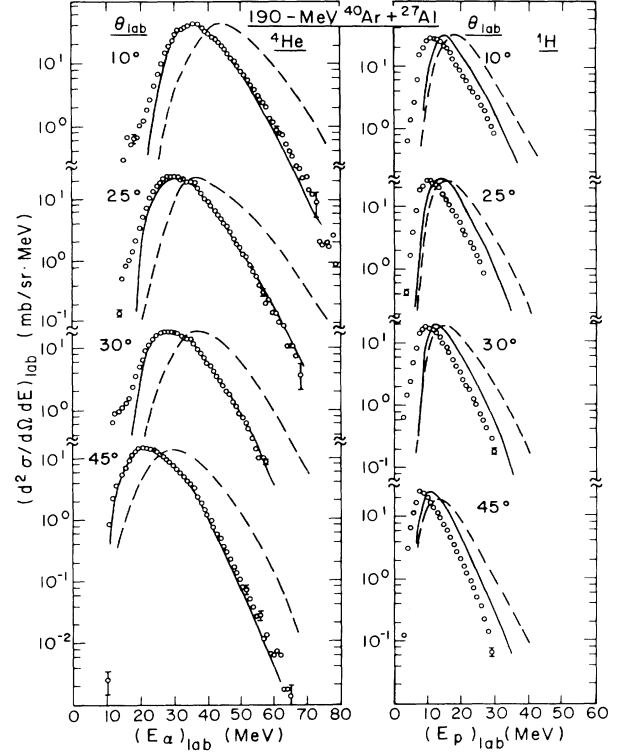


FIG. 2. Laboratory energy spectra of ^4He (left) and ^1H (right) from $^{40}\text{Ar} + ^{27}\text{Al}$ reactions. The points are experimental data and the curves are results from statistical model calculations for spherical nuclei (---) and deformed nuclei (—). See text for details.

spectra with statistical model calculations¹⁻³ using the evaporation-simulation code GANES.⁷ This code evaluates the relative probability of emitting a particle of given mass, charge, energy, and orbital angular momentum from a spherical nucleus with known mass, charge, excitation energy, and spin, into an angle whose direction is specified with respect to the emitter spin. Particle spectra and angular distributions are built by repeated event-by-event sampling of the relevant quantities in a Monte Carlo fashion.

As input for the calculations, we have used a triangular spin distribution in the entrance channel, $0 \leq l \leq l_{\text{crit}}$, and appropriate fusion barriers for the exit channels as taken from systematics.⁸ A value $l_{\text{crit}} = 46\hbar$ was derived from fusion cross-section data.⁶ Calculated results are shown as dashed curves in Fig. 2. Compared to the experimental data, the calculated spectra for both ^4He and ^1H are shifted to higher energies and are substantially broadened. Measured c.m. angular distributions for ^4He and ^1H are shown in Fig. 3; calculated angular distributions (dashed curves) display greater anisotropies than do the data (points). The calculated anisotropy is determined primarily by the ratio of the rotational energy (i.e., αJ^2) to the temperature,^{1-3,7} and as the spin zone is fixed by cross-section data, one might suspect that the large calculated anisotropy is due to the effective temperature. However, the dashed curves in Figs. 2 and 3 already represent first-

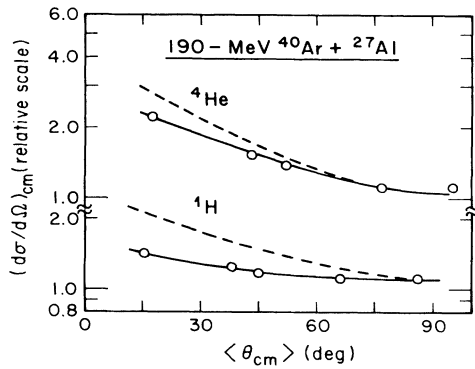


FIG. 3. Angular distributions of ${}^4\text{He}$ and ${}^1\text{H}$ in the c.m. system. The points are experimental data and the curves are statistical model calculations for spherical nuclei (---) and deformed nuclei (—). The calculated curves have been normalized to the data at 90° to illustrate the difference in anisotropies.

step emission for the evaporated particle, and hence the highest reasonable temperature. Particle emission very near the yrast line is not included in our calculations. Such particles could have subbarrier energies, but their large l values and low temperatures would lead to even larger predicted anisotropies.⁴ Within the constraints of a Fermi gas model and spherical nuclei, a problem clearly exists.

There are, in fact, two related but distinct difficulties. First, the effective emission barriers in the calculations must be substantially higher than those of the real nuclei. This causes the calculated spectra to appear at higher energies than the experimental spectra. Second, the spherical moments of inertia used in the calculations, when combined with the spin distribution required by the fusion cross section, produce larger angular anisotropies than observed. If significantly lower effective emission barriers are used,⁹ good fits can be obtained for the evaporation spectra, but the correspondence with observed fusion data⁸ for ${}^4\text{He}$ and ${}^1\text{H}$ would be lost. It is important to recognize that these effects are not peculiar to the evaporation code GANES. All statistical model codes use the same basic physics (empirical barriers or transmission coefficients from interactions between cold nuclei, Fermi gas level densities, three-dimensional coupling between emitter spin and exit channel spin). There are no substantial differences between quantum mechanical and semiclassical calculations in this context.¹⁰ Thus, any statistical model code which calculates particle evaporation from spherical nuclei will manifest similar behavior (unless masked by arbitrary radius parameters, moments of inertia, transmission coefficients, or equivalent internal quantities).

How can this dilemma be resolved? If the hot, rotating nuclei under consideration here are not spherical, but strongly deformed as has been suggested,^{5,11-13} then emis-

sion barriers would be lowered in directions of large radial extent, and the enlarged moments of inertia would reduce the angular anisotropies. We have pursued this approach by trying to fit the observed data with statistical model calculations for deformed nuclei.¹⁴ In these calculations, we have used a Cassini shape parameterization,¹⁵ and the root-mean-square spin of the emitting nucleus was fixed [$J_{\text{rms}} = (I_{\text{crit}}^2/2)^{1/2}$] by the fusion data. The nuclear potential was of Woods-Saxon form with diffuseness adjusted to match the fusion barrier for a spherical shape. The emission barriers were then controlled by the Coulomb-nuclear potential of the deformed nuclear shape.¹⁵ Only the shape and the mean excitation energy were varied, with the resulting "best fits" shown as the solid curves in Figs. 2 and 3. As can be seen, the ${}^4\text{He}$ spectra and anisotropies can be fit very well using the deformed nuclear model. The curves for the ${}^4\text{He}$ spectra in Fig. 2 were obtained with a near-prolate shape with axis ratio 2.4 and a mean excitation energy of 64 MeV (compared to an initial value of 91 MeV). Oblate shapes of similar axis ratio give nearly the same spectra for this system. The reduced effective excitation energy is reasonable, since ${}^4\text{He}$ (or ${}^1\text{H}$) emission can occur at any step of the evaporation cascade, and hence some excitation energy can be lost before the average ${}^4\text{He}$ (or ${}^1\text{H}$) emission step. However, the very large axis ratio required may imply that this simple deformation approach is unrealistic. The ${}^1\text{H}$ spectra on the right side of Fig. 2 were calculated with the same deformed shape and effective excitation energy as were used for the ${}^4\text{He}$ spectra. This calculation accounts for the anisotropies in Fig. 3 and gives some improvement in the calculated spectra compared to the spherical case. However, the predicted spectra are still at significantly higher energies than those observed. This result persists even if one sums calculated spectra from several temperatures (or emission steps), and extends the range of T_i values to less than 10^{-5} (the default cutoff in GANES). It appears that the angular distribution problem can be taken care of by invoking deformation, but the effective barrier lowering for ${}^1\text{H}$ is inadequate.

What must we conclude? Since simple symmetric deformations cannot reproduce the observed ${}^1\text{H}$ spectra, the good fits achieved with the ${}^4\text{He}$ data must not reveal the whole story. Clearly, some basic feature is missing from the statistical model descriptions which probably affects both ${}^1\text{H}$ and ${}^4\text{He}$ emissions. There must be a new ingredient which effectively increases the mean evaporation radius in a manner unattainable by symmetric deformations alone. We are attracted to the idea of fluctuations (or a tail) in the nuclear density distribution, whereby proton evaporation can occur from less dense regions than may be needed for ${}^4\text{He}$ cluster evaporation. Whatever the speculation, it is important that the questions raised here be seriously addressed, both theoretically and experimentally, in order that one may use statistical models as important benchmarks for studies of new frontiers at high energy and spin.

- ¹T. Ericson and V. Strutinski, Nucl. Phys. **8**, 284 (1958); **9**, 689 (1959).
- ²T. Ericson, Adv. Phys. **9**, 425 (1960).
- ³T. Dossing, Licentiat Thesis, University of Copenhagen, Denmark, 1977.
- ⁴J. R. Grover and J. Gilat, Phys. Rev. **157**, 802 (1967); **157**, 823 (1967).
- ⁵D. J. Moses *et al.*, Z. Phys. A **320**, 229 (1985).
- ⁶Fusion cross sections for similar systems are analyzed in P. Frobrich, Phys. Rep. **116**, 337 (1984). They were used with slight scaling from calculational systematics of W. W. Wilcke *et al.*, At. Data Nucl. Data Tables **25**, 289 (1980).
- ⁷N. N. Ajitanand *et al.*, Nucl. Instrum. Methods Phys. Res. Sect. A **243**, 111 (1986).
- ⁸L. C. Vaz and J. M. Alexander, Z. Phys. A **318**, 231 (1984).
- ⁹M. Kaplan, DOE Annual Report No. COO-3246-25, Carnegie-Mellon University, October 1985 (unpublished).
- ¹⁰L. C. Vaz *et al.*, Z. Phys. A **324**, 331 (1986).
- ¹¹R. K. Choudhury *et al.*, Phys. Lett. **143B**, 74 (1984); G. Nebbia *et al.*, *ibid.* **176B**, 20 (1986).
- ¹²M. Blann, Phys. Rev. C **21**, 1770 (1980); M. Blann and T. T. Komoto, *ibid.* **24**, 426 (1981).
- ¹³H. Ho *et al.*, Heidelberg report (unpublished).
- ¹⁴N. N. Ajitanand *et al.*, Phys. Rev. C **34**, 877 (1986).
- ¹⁵V. V. Pashkevich, Nucl. Phys. **A169**, 275 (1971).